Efficient production of the Nylon 12 monomer ω-aminododecanoic acid methyl ester from renewable dodecanoic acid methyl ester with engineered *Escherichia coli*

Nadine Ladkau[a,1], Miriam Assmann[a,2], Manfred Schrewe[a,b], Mattijs K. Julsing[a], Andreas Schmid[a,b,*], and Bruno Bühler[a,b,*]

[a] Laboratory of Chemical Biotechnology, Department of Biochemical and Chemical Engineering, TU Dortmund University, Emil-Figge-Strasse 66, 44227 Dortmund, Germany.

[b] Department of Solar Materials, Helmholtz Centre for Environmental Research – UFZ, Permoserstrasse 15, 04318 Leipzig, Germany.

doi:10.1016/j.ymben.2016.02.011

[1] Current address: Department of Chemistry, University College London, 20 Gordon Street, WC1H 0AJ London, UK.

[2] Current address: Institute of Technical Biocatalysis, Technical University Hamburg-Harburg, Denickestrasse 15, 21073 Hamburg, Germany

Highlights:

- Orthogonal pathway engineering for Nylon 12 production from renewables in *E. coli*
- Hydrophobic substrate uptake via outer membrane porin
- Coupling of transaminase catalysis to the pyruvate node via alanine dehydrogenase
- Strain robustness regarding toxicities and recombinant expression as crucial factor
- Respiration-linked alcohol oxidation improves flux and minimizes by-product formation

Corresponding authors:

Phone: +49 341 235 1286, Fax: +49 341 235 451286, E-mail: andreas.schmid@ufz.de;

Phone: +49 341 235 4687; Fax: +49 341 235 451286, E-mail: bruno.buehler@ufz.de

Summary

The expansion of microbial substrate and product scopes will be an important brick promoting future bioeconomy. In this study, an orthogonal pathway running in parallel to native metabolism and converting renewable dodecanoic acid methyl ester (DAME) via terminal alcohol and aldehyde to 12-aminododecanoic acid methyl ester (ADAME), a building block for the high-performance polymer Nylon 12, was engineered in *Escherichia coli* and optimized regarding substrate uptake, substrate requirements, host strain choice, flux, and product yield. Efficient DAME uptake was achieved by means of the hydrophobic outer membrane porin AlkL increasing maximum oxygenation and transamination activities 8.3 and 7.6-fold, respectively. An optimized coupling to the pyruvate node via a heterologous alanine dehydrogenase enabled efficient intracellular L-alanine supply, a prerequisite for self-sufficient whole-cell transaminase catalysis. Finally, the introduction of a respiratory chain-linked alcohol dehydrogenase enabled an increase in pathway flux, the minimization of undesired overoxidation to the respective carboxylic acid, and thus the efficient formation of ADAME as main product. The completely synthetic orthogonal pathway presented in this study sets the stage for Nylon 12 production from renewables. Its effective operation achieved via fine tuning the connectivity to native cell functionalities emphasizes the potential of this concept to expand microbial substrate and product scopes.

Keywords: orthogonal pathway engineering, in vivo cascade biocatalysis, substrate uptake, Nylon 12, renewable plastics.

Chemical compounds studied in this article:

Methyl dodecanoate (PubChem CID: 8139); Methyl 12-hydroxydodecanoate (PubChem CID: 522424); Dodecanedioic acid monomethyl ester (PubChem CID: 231998); Methyl 12-aminododecanoate (PubChem CID: 3665980)

1. Introduction

Synthetic polyamides offer excellent chemical and physical properties for various applications as packing materials and parts in the automotive, construction, and medical industries (Carole et al., 2004; Schmitz and Schepers, 2004). Important representatives of the group of aliphatic polyamides are Nylon 6, 6.6, 6.12, 11, and 12 (Palmer, 2001). Nylon 12 constitutes a high performance polymer featuring extraordinary heat, abrasion, chemical, UV, and scratch resistance (Evonik Industries, 2015). Typically, Nylon 12 is produced from the monomer ω-laurolactam, of which the chemical synthesis is initiated by the trimerization of 1,3-butadiene originating from steam cracking of crude oil (Dachs and Schwartz, 1962; Franke and Müller, 1964). However, at times of decreasing crude oil resources, increasing concerns about process safety, and rising negative economic and environmental implications of crude oil use, the substitution of petrochemical with bio-based synthesis routes becomes more and more interesting.

Approaches involving the biotechnological production of polymer building blocks for, *e.g.*, Nylons (Curran et al., 2013; Kind et al., 2014; Niu et al., 2002) or polyesters (Lee et al., 2005) synthesis, typically are based on renewable resources and make use of microbes as production organisms. Systems biotechnology and metabolic engineering thereby facilitated the design of such whole-cell catalysts and enabled productivity and yield enhancements via the genetic modification of native microbial pathways and their regulation.

The design and construction of non-natural, heterologous and in this sense orthogonal pathways consisting of enzymes originating from different pathways/strains and running as separate synthetic modules in parallel to native metabolism (Oberleitner et al., 2013; Schrewe et al., 2013b; Song et al., 2013) can be considered a novel metabolic engineering approach to enlarge the substrate and product scope of microbial bioprocesses. However, the hitherto poor performance of such pathways and their coupling to the microbial physiology represent major

challenges, which remain to be tackled. Recently, we combined oxygenase and transaminase catalysis in such an orthogonal pathway for the conversion of plant oil derived dodecanoic acid methyl ester (DAME) to 12-aminododecanoic acid methyl ester (ADAME), a monomer suitable for Nylon 12 synthesis (Schrewe et al., 2013b). ADAME was produced in *E. coli* via a three-step cascade, in which terminal DAME hydroxylation and alcohol oxidation both catalyzed by the alkane monooxygenase AlkBGT from *Pseudomonas putida* GPo1 were followed by terminal amination by means of the *Chromobacterium violaceum* ω-transaminase (CV2025) (Fig. 1). Thereby, dodecanedioic acid monomethyl ester (DDAME) was formed as a major by-product.

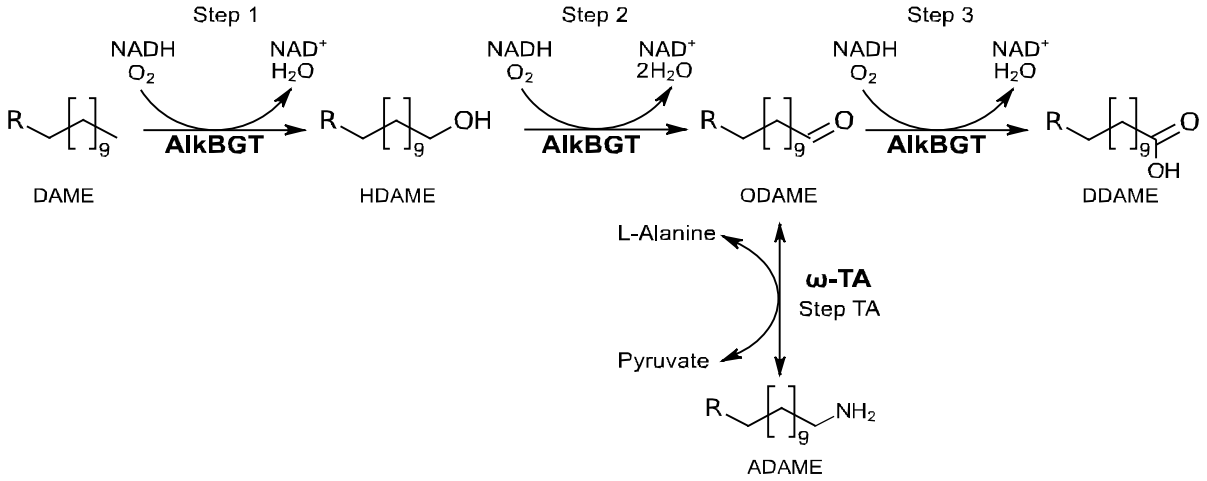

Fig. 1: Terminal oxy- and aminofunctionalization of DAME. AlkBGT, alkane monooxygenase; ω-TA, ω-transaminase CV2025; DAME, dodecanoic acid methyl ester; HDAME, 12-hydroxydodecanoic acid methyl ester; ODAME, 12-oxododecanoic acid methyl ester; DDAME, dodecanedioic acid monomethyl ester; ADAME, 12-aminododecanoic acid methyl ester; R, $COOCH_3$.

Limited substrate uptake into the cells, the necessity to feed L-alanine as cosubstrate for the transamination reaction, and by-product formation have been identified as critical factors. This study reports the redesign of the whole-cell catalyst for the efficient conversion of DAME to ADAME via orthogonal pathway and metabolic engineering. Approaches include the introduction of the outer membrane protein AlkL, which has been shown to enhance

hydrophobic substrate uptake over the outer membrane of recombinant *E. coli* (Cornelissen et al., 2013; Julsing et al., 2012), L-alanine supply via a heterologous alanine dehydrogenase making use of intracellular alanine and pyruvate pools, and the increase of the flux through the orthogonal pathway via the introduction of a heterologous alcohol dehydrogenase catalyzing irreversible alcohol oxidation. Furthermore, different *E. coli* host strains were evaluated regarding their ability to cope with the non-natural substrates and intermediates and their potential to efficiently synthesize the Nylon 12 monomer ADAME from renewables.

2. Materials and Methods

2.1 Chemicals

DAME (99.8%), 12-hydroxydodecanoic acid methyl ester (HDAME; ≥95%), 12-oxododecanoic acid methyl ester (ODAME; ≥95%), ADAME (99.3%), and 12-aminododecanoic acid (96%) were obtained from Evonik Degussa GmbH (Marl, Germany). All other chemicals used in this work were obtained from Carl Roth GmbH + Co KG (Karlsruhe, Germany), Merck KGaA (Darmstadt, Germany), Sigma Aldrich (Steinheim, Germany), and TCI Europe (Zwijndrecht, Belgium) in the highest purity available.

2.2 Strains, plasmids, and cultivation

Strains and plasmids used in this work are listed in Table 1. *E. coli* DH5α was used for cloning purposes and *E. coli* JM101, *E. coli* W3110, and *E. coli* BL21 (DE3) for biotransformation studies. Recombinant strains were obtained by introduction of plasmid DNA into the host strains via electroporation (2.5 kV, EquiBio Easyjet Pima Ashford UK). Transformants were selected via their antibiotic resistance.

Cultivations were carried out at 37 °C in LB medium (Sambrook, 2001) and at 30 °C for cultures in M9* minimal medium (Panke et al., 1999) supplemented with US^{Fe} trace element solution (Bühler et al., 2003) and 0.5% (w/v) glucose. For cultivation, a Multitron orbital shaker (Infors

HT, Bottmingen, Switzerland) was used at 200 rpm. Where appropriate, antibiotics were added: 50 µg mL^{-1} kanamycin (Km) and/or 34 µg mL^{-1} chloramphenicol (Cam). Solid media contained 1.5% (w/v) agar. Stock cultures were prepared by addition of 200 µL 50% (v/v) glycerol to 800 µL over-night grown LB cultures and stored at −80 °C.

Table 1: *E. coli* strains and plasmids

	Characterization	References
E. coli strains		
BL21 (DE3)	F^-, *ompT*, *hsdSB* (r_B^- m_B^-), λ(DE3 [*lacI* *lac*UV5 T7 gene *1 Sam7* Δ*nin5*])	(Studier and Moffatt, 1986)
DH5α	F^-, *endA1*, *gln*V44, *thi−1*, *recA1*, *relA1*, *gyrA96*, *deoR*, *supE44*, Φ80d*lac*ZΔM15 Δ(*lacZYA−argF*)-U169, *hsd*R15 (r_K^- m_K^+), λ^-	(Hanahan, 1983)
JM101	*supE*, *thi* Δ(*lac−proAB*) F' [*traD36* $proAB^+$ $lacI^q$ *lacZ* ΔM15]	(Messing, 1979)
W3110	F^{-1} λ^-, rph−1, *IN*(*rrnD−rrnE*)1	(Bachmann, 1987)
Plasmids		
pTA	pACYCDuet−1 derivative, P15A *ori*, T7-promoter, carries *cv2025* containing a 6xHis-tag and the N-terminal spacer AGCCAGGATCCGAATTCGAGCTCA, Cam^r	(Schrewe et al., 2013b)
pBTL10	derivative of alkane responsive broad-host-range vector pCom10 (Smits et al., 2001), *col*E1 *ori*, carries *alkBFGL* and *alkST*, Km^r	(Julsing et al., 2012)
pBTLJ10	pCom10 derivative (Smits et al., 2001), *col*E1 *ori*, carries *alkBFGJL* and *alkST*, Km^r	(Schrewe et al., 2014)
pCom10alkL	pCom10 derivative (Smits et al., 2001), carries *alkL* and *alkS*, Km^r	(Julsing et al., 2012)
placI	P15A *ori*, carries *lacI*, Cam^r	Merck KGaA, (Darmstadt, Germany)
pJ281	P15A *ori*, *lacUV5* promoter, carries *alaD* and *cv2025* (codon usage changed: leucine codon changed from ctg to ctc), Km^r	Evonik Degussa (Marl, Germany)
pAlaDTA[1]	placI derivative, *lacUV5* promoter, carries *alaD* and *cv2025*, Cam^r	This study

[1] The *alaD* and *cv2025* gene sequences are given in the supplementary material I and II.

2.3 Construction of pAlaDTA expression vector

T4 Ligase, thermosensitive Alkaline Phosphatase AP^{TM}, and restriction endonucleases were purchased from Fermentas GmbH (St. Leon-Rot, Germany) and used according to the suppliers' protocols. All primers were purchased from Eurofins MWG (Ebersberg, Germany). Plasmid DNA was isolated using the peqGOLD Miniprep Kit I (PEQLAB Biotechnology GmbH, Erlangen, Germany). The *alaD-cv2025* operon (including the *lac*UV5 promoter and the *rrnB*1 terminator) was amplified via PCR from the plasmid pJ281, which was kindly provided by Evonik Degussa (Marl, Germany), using the primers 5'-GCAGGGCCTGTCTCGGTCGATCATTCAGC-3' containing an *EcoO109*I restriction site and 5'-CGTAGCCTGAGGCCTGAATATGGCTCATA-3' containing an *Eco81*I site. The PCR product was cut with *EcoO109*I/*Eco81*I, phosphorylated, and ligated into the placI vector digested with the same enzymes. Successful cloning yielding the plasmid pAlaDTA was verified via sequencing of the insert region (MWG Eurofins, Ebersberg, Germany).

2.4 Biotransformation procedure

For precultivation, 5 mL LB medium were inoculated with a single colony from an LB agar plate and cultivated for 8 h. 500 µL of the LB culture were used to inoculate 50 mL M9* medium, followed by overnight incubation. Subsequently, 100 mL M9* medium were inoculated with the M9* preculture to a biomass concentration of 0.03 $g_{CDW}\ L^{-1}$. The cells were grown to a cell concentration of 0.08 $g_{CDW}\ L^{-1}$ and induced with 1 mM isopropyl-β-thiogalactopyranoside (IPTG) (pTA or pAlaDTA containing *E. coli* strains) and/or with 0.025% (v/v) dicyclopropylketone (DCPK) (*E. coli* strains harboring pCom10alkL, pBTL10, or pBTJL10) for 5 h before the cells were harvested and used for whole-cell biotransformations which were performed as described before (Schrewe et al., 2013b). The transaminase activity was determined in the same way except that the biotransformation buffer (Kpi, 50 mM phosphate buffer containing 1% (w/v) glucose, pH 7.4) contained either no supplement, 50 mM

L-alanine, or 5 - 15 g L^{-1} NH_4Cl. Activities were calculated in U g_{CDW}^{-1}, where 1 U is defined as 1 µmol product formed per min.

2.5 Analytic procedures

Analysis of DAME and its oxygenation and transamination products was carried out via gas chromatography using a Thermo Scientific Ultra™ Chromatograph (Waltham, MA) and reversed phase high pressure liquid chromatography using a VWR Hitachi LaChrome Elite HPLC system (Darmstadt, Germany) equipped with a Luna C8(2) column (4.6 x 150 mm, 5 µm, 100Å, Phenomenex, Aschaffenburg, Germany) and connected to a charged aerosol Corona detector (ESA Biosciences Inc, Chelmsford, MA) as described before (Schrewe et al., 2013b).

Cell concentrations were determined via measurement of the optical density at 450 nm (OD_{450}) (Libra S11 spectrophotometer; Biochrom Ltd., Cambridge, United Kingdom) with an OD_{450} of 1 corresponding to 0.166 g_{CDW} L^{-1} (Blank et al., 2008). SDS-PAGE analysis was performed according to the protocol of (Laemmli, 1970).

3. Results

3.1 AlkL boosts flux through the orthogonal pathway

Recently, the multistep conversion of renewable DAME to ADAME using whole cells of *E. coli* BL21 (DE3) (pTA, pBT10) was reported (Schrewe et al., 2013b). The poor water solubility of DAME and substrate uptake over the cell membrane were discussed as main factors restricting production rates (Schrewe et al., 2013b). Julsing et al. (2012) reported that the oxygenation activity of recombinant *E. coli* for hydrophobic hydrocarbons can be drastically increased via the introduction of the outer membrane protein AlkL originating from the alkane degradation operon of *P. putida* GPo1. In this study, the outer membrane protein AlkL was introduced into recombinant *E. coli* BL21 (DE3) (pTA) and *E. coli* BL21 (DE3) (pTA, pBT10)

to test its effect on the transamination reaction and the multistep conversion of DAME to ADAME, respectively.

With ODAME as substrate, cells containing AlkL showed 8-times higher specific transamination activities as compared to cells without AlkL (Table 2). Specific rates for oxygenase-catalyzed DAME and HDAME-oxidation were increased 8.1- and 6.8-fold, respectively, considering the full reaction sequence from DAME to ADAME. The transamination reaction, with a 7.3-fold increase in specific rate, was significantly favored over the competing oxidation of ODAME to DDAME (3.4-fold increase), resulting in the accumulation of 0.55 mM ADAME as main product within 60 min (Fig. 2). Hydrolysis of HDAME, ADAME, and DDAME to their corresponding acids 12-hydroxydodecanoic acid (15% of total alcohol), 12-aminododecanoic acid (2%), and 12-dodecandioic acid (22%) was observed during the biotransformation (for details see supplementary material, Fig. S1), as it also has been observed before (Schrewe et al., 2013b). As expected, introduction of the outer membrane protein AlkL into the whole-cell biocatalyst resulted in increased conversion rates for the multistep bioconversion of DAME to ADAME.

Table 2: Effect of AlkL on specific activities of recombinant *E. coli* BL21 (DE3) for ADAME formation from ODAME or DAME.

Plasmid(s)	Substrate	Step 1	Step 2	Step 3	Step TA	Reference
pTA	ODAME		−17±1.9[1]	0.8±0.1[1]	82±2.4	(Schrewe et al., 2013b)
pTA, pBT10	DAME	2.9±0.2	2.4±0.1	1.4±0.1	1.5±0.1	(Schrewe et al., 2013b)
pTA, pCom10alkL	ODAME		−32±0.7[1]	n.d.	623±26	This study
pTA, pBTL10	DAME	23.6±0.6	16.3±1.1	4.8±0.9	11.0±0.4	This study

Bioconversions were performed under the following conditions: 2.5 mM substrate, 0.5-1.5 $g_{CDW}\ L^{-1}$ of recombinant *E. coli* BL21 (DE3), and 50 mM L-alanine. Specific activities are given in U g_{CDW}^{-1} (1 U = 1 µmol min^{-1}). The reaction steps are denominated as defined in Fig. 1.
n.d. – not detected.
[1]Host intrinsic ODAME reduction and oxidation.

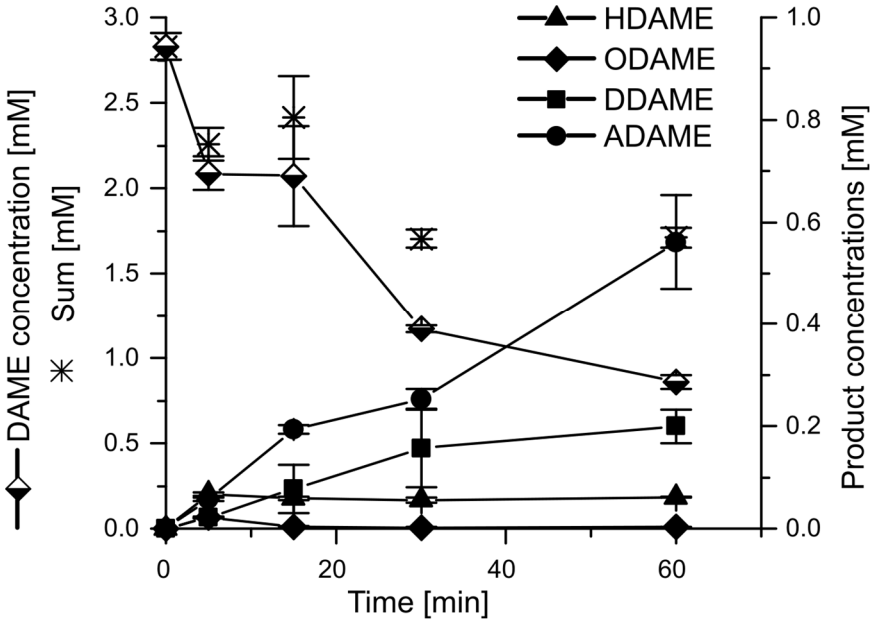

Fig. 2: Terminal oxy- and aminofunctionalization of DAME with *E. coli* BL21 (DE3) (pTA, pBTL10). Cell concentration applied: 1.25 g_{CDW} L^{-1}. Kpi buffer was supplemented with 50 mM L-alanine. The concentrations of hydrolysis products (*i.e.*, 12-hydroxydodecanoic acid, dodecanedioic acid, and 12-aminododecanic acid) were summed up with those of the corresponding esters. See supporting information about details on ester hydrolysis. Abbreviations are as given in the legend of Fig. 1.

3.2 *In vivo* supply of the transamination cosubstrate alanine

L-alanine is a preferred cosubstrate for CV2025 and typically has been used for *in vitro* applications of this transaminase (Kaulmann et al., 2007; Sattler et al., 2012). Native L-alanine biosynthesis in *E. coli* BL21 (DE3) (pTA) was found insufficient to support efficient ODAME transamination, for which the ADAME yield on biomass was increased from 0.01 to 0.59 mmol g_{CDW}^{-1} when 50 mM L-alanine was provided (Schrewe et al., 2013b). In order to boost L-alanine formation from the pyruvate released during transamination or formed during glucose catabolism, the alanine dehydrogenase AlaD from *B. subtilis* was introduced into the microbial host strain. This enzyme was chosen, as it has been reported to efficiently support *in vitro* transaminase catalysis via alanine regeneration from pyruvate (Sattler et al., 2012). To evaluate "self-sufficient" *in vivo* transamination, the combination of *B. subtilis* AlaD and CV2025 was tested in different *E. coli* host strains, *i.e.*, *E. coli* W3110, *E. coli* JM101, and *E. coli* BL21 (DE3), either with or without AlkL (Table 3). These strains were chosen based on the following

reasons: *E. coli* W3110 has been shown to be a potent host for AlkBGT-catalysis (Schrewe et al., 2011), as it is able to form additional membrane structures upon *alkB*-overexpression (Nieboer et al., 1996); *E. coli* JM101 has been described as a robust host for various oxygenase-catalyzed reactions (Bühler et al., 2000; Kuhn et al., 2013; Park et al., 2006); and *E. coli* BL21 (DE3) is well established for recombinant gene expression and has been used for *alkBGT* and *cv2025* co-expression enabling the proof of concept for the multistep conversion of DAME to ADAME (Schrewe et al., 2013b).

Table 3: Specific ODAME transamination activities of *E. coli* strains containing AlaD and CV2025 with and without AlkL.

		Specific activities of *E. coli* strains [U g_{CDW}^{-1}]		
Plasmids	Ammonium sources	BL21 (DE3)	W3110	JM101
pAlaDTA	none	0.4±0.1	0.4±0.1	0
	50 mM Alanine	29.6±2.7	29.5±5.9	30.1±1.8
	5 g/L NH_4Cl	14.6±1.6	10.7±0.1	7.4±0.7
	10 g/L NH_4Cl	20.3±2.9	16.3±0.7	8.7±0.8
	15 g/L NH_4Cl	22.2±1.0	17.9±0.9	11.0±0.4
pAlaDTA, pCom10alkL	none	0	0	0
	50 mM Alanine	198±8.0	253±3.0	210±7.3
	5 g L^{-1} NH_4Cl	10.2±0.4	17.6±0.2	9.1±0.5
	10g L^{-1} NH_4Cl	9.4±1.0	17.7±0.8	11.3±0.9
	15 g L^{-1} NH_4Cl	12.3±0.8	17.1±0.6	11.9±0.6

Bioconversions were performed with $0.8 - 1.35$ g_{CDW} L^{-1} of resting cells in Kpi buffer containing various ammonium sources and 2.5 mM ODAME. Specific activities are given in U g_{CDW}^{-1} (1 U = 1 µmol min^{-1}).

As expected, ODAME was converted to ADAME at very low specific rates of $0 - 0.4$ U g_{CDW}^{-1} in negative control reactions without ammonium source in the reaction buffer. Specific transamination rates between 7.4 and 22.2 U g_{CDW}^{-1} were observed upon addition of 5 to 15 g L^{-1} NH_4Cl to the reaction buffer, indicating that the introduction of AlaD improved intracellular L-alanine availability in the absence of alanine in the medium.

Recombinant *E. coli* BL21 (DE3) without AlkL showed the highest transamination activity with NH_4Cl as ammonium source. A positive effect of the substrate uptake facilitator AlkL on the ODAME conversion rates was only observed upon alanine addition, where ADAME

formation rates increased by a factor of 6.6 – 8.5. With NH_4Cl, AlkL did not significantly improve transamination rates in any of the strains. Apparently, the transaminase activity was limited by alanine supply via AlaD rather than ODAME availability.

Facilitated substrate and intermediate uptake via AlkL can impair the biocatalyst stability due to toxification leading to a fast loss in energy (e.g., NADH)-dependent bioconversion activity (Julsing et al., 2012; Schrewe et al., 2014). With NH_4Cl as N-source, *E. coli* BL21 (DE3) (pAlaDTA, pCom10alkL) showed lower transamination activities than *E. coli* BL21 (DE3) (pAlaDTA), while increased transamination rates were observed with L-alanine. The AlaD reaction is tightly linked to the cell's carbon and energy metabolism via NADH, pyruvate, and the uptake of ammonium, whereas the transamination reaction only depends on ODAME and L-alanine availability. Thus, the higher CV2025-rates in presence of alanine can be explained by increased intracellular ODAME availability via AlkL. With NH_4Cl, however, the energy metabolism-dependent AlaD reaction in the BL21 (DE3) strain and thus indirectly also the CV2025 reaction may have been compromised by toxic effects caused by facilitated ODAME transfer over the outer membrane mediated by AlkL. *E. coli* JM101 and *E. coli* W3110 showed similar transamination rates in the presence and absence of AlkL, obviously coping better with elevated intracellular ODAME concentrations.

In comparison to the experiments performed with *E. coli* BL21 (DE3) (pTA) and L-alanine addition (Table 2), specific ODAME transamination rates (82 and 623 U g_{CDW}^{-1} without and with AlkL, respectively) were between 2.8- and 3.1-fold lower with recombinant *E. coli* BL21 (DE3) carrying the plasmid pAlaDTA (29.6 and 198 U g_{CDW}^{-1}, Table 3). This difference can be explained by lower CV2025 amounts formed in *E. coli* BL21 (DE3) (pAlaDTA) as compared to *E. coli* BL21 (DE3) (pTA) (see supplementary material, Fig. S4), in which the *cv2025* gene is the first and not the second gene on the operon controlled by a stronger promoter system (T7

instead of *lacUV5*, see Table 1). The weaker *lacUV5* promoter was chosen to enable efficient co-expression of multiple genes (see below).

To conclude, the coupling of AlaD and CV2025 *in vivo* has been successfully achieved in all tested recombinant *E. coli* strains enabling efficient ODAME transamination independently of an external L-alanine feed. Furthermore, the experiments indicated that the investigated host organisms differ regarding their robustness towards an AlkL-mediated elevation of the substrate load.

3.3 Multistep biotransformation of DAME in the presence of AlkL and AlaD

As the next step, the combination of AlkL and AlaD was tested regarding its effect on the multistep conversion of DAME to ADAME. For this purpose, recombinant *E. coli* BL21 (DE3), *E. coli* W3110, and *E. coli* JM101 harboring the plasmids pAlaDTA and pBTL10 were employed in the presence of L-alanine or NH_4Cl (Fig. 3).

In the presence of L-alanine, the strains W3110 and JM101 showed similar maximum activities for all reaction steps with ADAME and DDAME as main products and similar product yields on biomass after 60 min. *E. coli* BL21 (DE3) showed lower activities and yields and a higher HDAME product share. As observed for ODAME conversion (Table 3), lower transamination rates were obtained when NH_4Cl was used as ammonium source. Increasing the ammonium concentration did not result in increased maximum ADAME formation rates and yields with the BL21 (DE3) strain, which, in contrast, was the case with *E. coli* W3110 and especially *E. coli* JM101 (Fig. 3B). With the latter two strains, the intracellular alanine supply via AlaD again appeared to limit amine formation and directly influenced the product formation pattern. Increasing ammonium concentrations resulted in increasing amine to acid ratios.

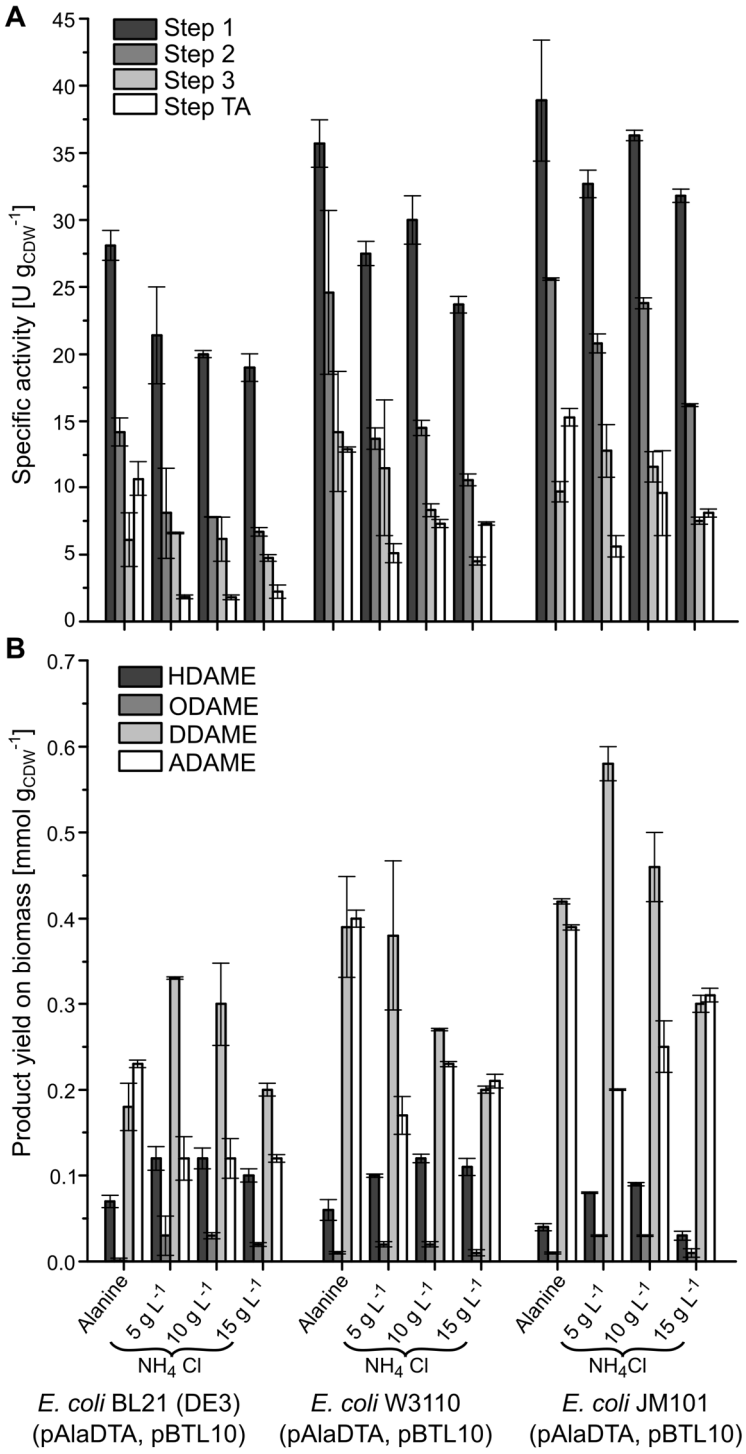

Fig. 3: Maximum specific activities (U g_{CDW}^{-1}) (A) and product yields on biomass (mmol g_{CDW}^{-1}) (B) obtained in bioconversions of 2.5 mM DAME performed for 60 min with *E. coli* strains BL21 (DE3), W3110, and JM101 containing pAlaDTA and pBTL10. The same procedure as for the experiment shown in Fig. 2 was followed and maximum activities given in panel A refer to the time intervals with the highest respective activities. Cell concentration applied: 0.63 - 1.0 g_{CDW} L^{-1}. Kpi buffer was supplemented with 50 mM L-alanine or 5, 10, or 15 g L^{-1} NH_4Cl. Detected amounts of the hydrolysis products (*i.e.*, 12-hydroxydodecanoic acid, dodecanedioic acid, and 12-aminododecanoic acid) were summed up with those of corresponding esters. Reaction step nomenclature and abbreviations are as given in the legend of Fig. 1.

In contrast to their higher oxygenation and transamination activities and product yields on biomass, *E. coli* W3110 and *E. coli* JM101 synthesized AlkB and CV2025 to slightly lower levels as compared to *E. coli* BL21 (DE3) (see supplementary material Figs. S4, S5, S6). Thus, either not all enzymes formed were active or, as already inferred from the reduced AlaD-limited transamination rates in the presence of AlkL in *E. coli* BL21 (DE3) (Table 3), toxic substrate/product levels compromised cell metabolism and thus pyruvate supply, NADH regeneration, and/or ammonium uptake to a greater extent in *E. coli* BL21 (DE3). Since *E. coli* JM101 performed slightly better than *E. coli* W3110 with NH_4Cl as ammonium source and the latter strain showed drastically reduced growth after transformation with both plasmids (for further information see supplementary material, Table S1), *E. coli* JM101 was chosen as the most suitable host strain.

3.4 The alcohol dehydrogenase AlkJ facilitates ADAME synthesis

ODAME transamination by cells with and without AlkL in the outer membrane revealed a direct dependence of respective activities on intracellular ODAME availability (Table 3). The multistep conversion of DAME involving AlkL, AlkBGT, and CV2025 resulted in the parallel accumulation of DDAME and ADAME, whereas only very low amounts of ODAME were detected pointing to ODAME limitation (Figs. 2 and 4A). To support ODAME formation, the heterologous pathway was amended by the NAD(P)H independent alcohol dehydrogenase AlkJ from *P. putida* GPo1. AlkJ transfers electrons to the electron transport chain (Kirmair and Skerra, 2014) and thus catalyzes irreversible alcohol oxidation (Schrewe et al., 2014).

Whereas the bioconversion of DAME with *E. coli* JM101 (pAlaDTA, pBTL10) resulted in similar specific DDAME and ADAME formation rates and yields (Fig. 4A and B), the introduction of AlkJ effected a clear shift towards the desired amine formation (Fig. 4C and D). This effect involved increased ODAME (Step 2) and ADAME (Step TA) formation rates and slightly decreased DDAME (Step 3) formation rates.

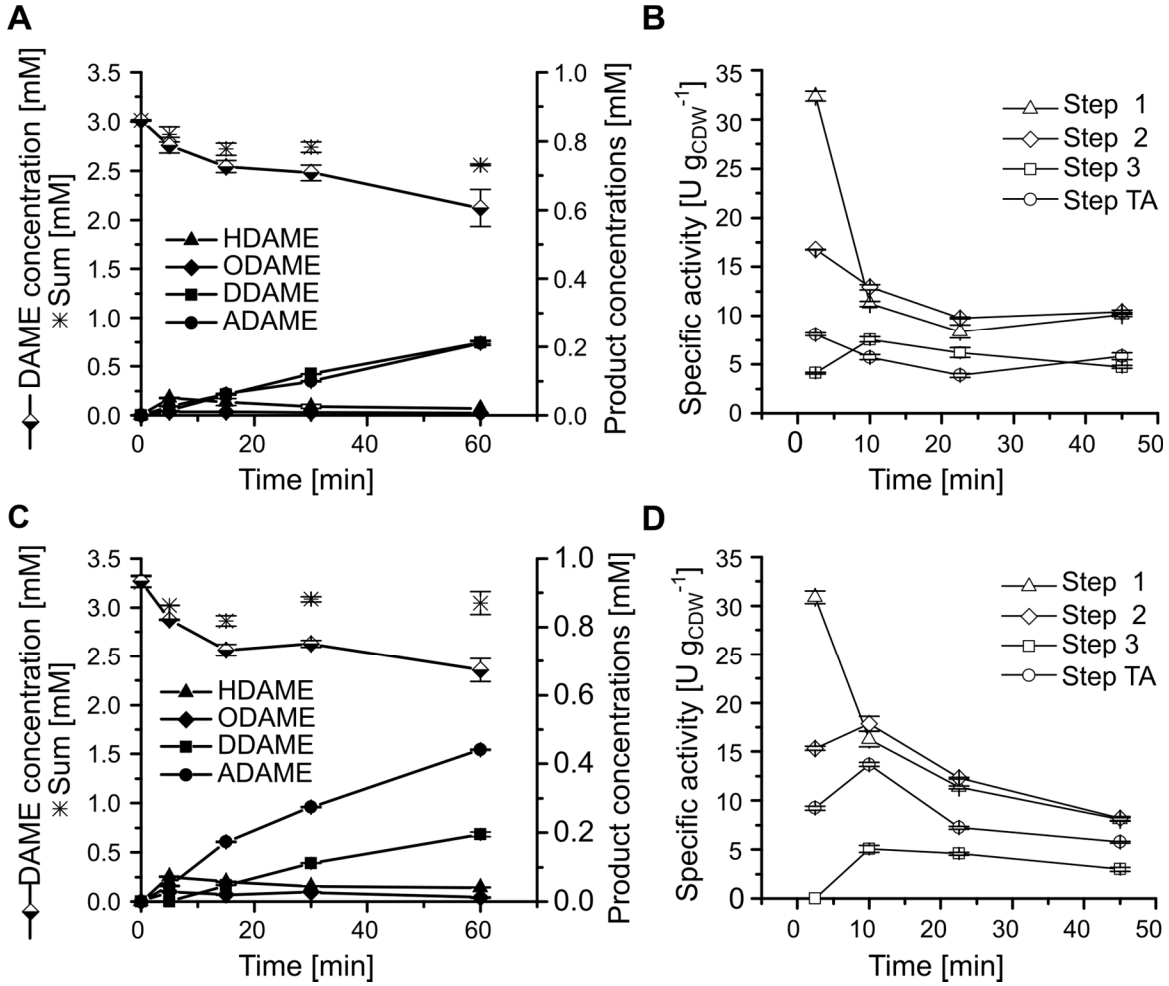

Fig. 4: DAME bioconversion with *E. coli* JM101 (pAlaDTA, pBTL10) (0.64 g_{CDW} L^{-1}; A and B) and *E. coli* JM101 (pAlaDTA, pBTJL10) (0.93 g_{CDW} L^{-1}; C and D). The course of substrate, intermediate, and product concentrations (A and C) and of specific activities (B and D) is given. Kpi buffer was supplemented with 15 g L^{-1} NH_4Cl. The concentrations of hydrolysis products (i.e., 12-hydroxydodecanoic acid, dodecanedioic acid, and 12-aminododecanic acid) were summed up with those of the corresponding esters. See supplementary material, Figs. S2 and S3 about details on ester hydrolysis. Reaction step nomenclature and abbreviations are as given in the legend of Fig. 1.

The increase of the fluxes through the orthogonal ADAME synthesis pathway as it was achieved via the introduction of AlkL and AlkJ and the establishment of intracellular alanine supply via AlaD now enables the production of ADAME as main product without external alanine feeding. The metabolically engineered recombinant strain *E. coli* JM101 (pAlaDTA, pBTL10) represents an excellent basis for the establishment of a process for Nylon 12 production from renewable DAME.

352 **4. Discussion**

353 **4.1 The role of hydrophobic substrate uptake in ADAME synthesis**

354 Whole-cell catalyzed ADAME synthesis from plant oil derived DAME suffers from substrate
355 uptake limitation over the cellular membranes (Schrewe et al., 2013b). The hydrophilic
356 lipopolysaccharide layer on the surface of microbial cells and the hydrophilic nature of typical
357 outer membrane pores constitute a barrier for larger, hydrophobic compounds, whereas the
358 cytoplasmic membrane represents a barrier for hydrophilic molecules (Chen, 2007; Leive,
359 1974; Nikaido, 2003). Substrate uptake into microbial cells can be enhanced via the
360 introduction of transport proteins or pores into cellular membranes. As reported recently, the
361 outer membrane protein AlkL from *P. putida* GPo1 has been proven to enable efficient transfer
362 of alkanes, fatty acids, fatty acid methyl esters, and terpenes over the outer cell membrane,
363 boosting the hydroxylation activity of recombinant *E. coli* towards such hydrophobic or
364 amphiphilic compounds (Cornelissen et al., 2013; Julsing et al., 2012; Scheps et al., 2013). In
365 the present work, the incorporation of AlkL into the investigated *E. coli* strains resulted in
366 increased specific rates for ODAME transamination and for the flux through the orthogonal
367 pathway from DAME to ADAME. However, boosted uptake via AlkL has been observed to
368 cause/intensify substrate/product toxicity (Julsing et al., 2012; Schrewe et al., 2014). Similarly,
369 using *E. coli* BL21 (DE3) as host strain, high AlkL levels appeared to hamper AlaD-driven
370 ODAME transamination and orthogonal pathway performance (Table 3, Fig. 3).
371 Substrate/product toxicity might become a critical issue for process development and scale up
372 involving higher substrate and product concentrations. Typically, substrate and product
373 toxification can be prevented by regulated substrate addition and *in situ* product removal, *e.g.*,
374 via evaporation, extraction, permeation, immobilization, or precipitation (Stark and von
375 Stockar, 2003).

4.2 AlaD – linking central carbon metabolism and the orthogonal pathway enabled intracellular L-alanine supply for efficient transamination

E. coli is able to produce L-alanine intracellularly. On average, *E. coli* produces L-alanine at rates of around 0.73 mmol g_{CDW}^{-1} h^{-1} (12.2 U g_{CDW}^{-1}) during exponential growth at 37 °C in glucose containing minimal medium (Pramanik and Keasling, 1997). However, such native L-alanine synthesis was not sufficient to efficiently support ODAME transamination resulting in only poor ADAME formation from DAME with resting *E. coli* BL21 (DE3) (pTA, pBTL10) (Schrewe et al., 2013b). Connecting the orthogonal pathway to the central carbon metabolism via the *B. subtilis* alanine dehydrogenase AlaD to enhance L-alanine formation from pyruvate enabled efficient transamination in alanine-free medium. However, with ODAME as well as DAME as substrate, alanine supply via AlaD still limited the transamination reaction, as it can be deduced from the higher rates achieved when L-alanine was provided externally. AlaD-catalysis strictly depends on the availability of ammonium. Accordingly, the ammonium concentration in the reaction medium was found to be critical regarding orthogonal pathway performance. Similarly, L-alanine production in *E. coli* involving *B. sphaericus* AlaD was reported to cease at low ammonium concentrations and could be sustained by pulsing 15 g L^{-1} NH_4Cl (Lee et al., 2004). For *B. subtilis* AlaD, a high Michaelis-Menten constant towards NH_4^+ has been reported (K_M = 38 mM, determined *in vitro* at 25 °C and pH 8; Yoshida and Freese, 1965). This, in combination with the intracellular competition for NH_4^+, *e.g.*, with glutamate dehydrogenase, can be considered critical for efficient *in vivo* transamination necessitating a tight control of ammonium levels in the medium or making AlaD a target for respective protein engineering.

Next to NH_4^+, AlaD-catalysis also interferes with the intracellular pyruvate pool. In principle, one molecule of pyruvate is released upon ODAME amination and can be recycled to L-alanine via AlaD. However, pyruvate is a key metabolite of the central carbon metabolism, for which

several host intrinsic enzyme reactions are competing. Thus, further strain engineering, *i.e.*, the knockout or knockdown of competing pyruvate consuming reactions, may improve AlaD- and transaminase catalysis. Such a strategy has been followed for alanine production by *E. coli* overproducing recombinant AlaD. The knockout of pyruvate-formatelyase, pyruvate oxidase, phosphoenolpyruvate synthase, lactate dehydrogenase, as well as components of the pyruvate dehydrogenase complex resulted in the production of up to 88 g L^{-1} D-/L-alanine from glucose in a fed-batch-based bioprocess (Smith et al., 2006). However, TCA cycle activity and NAD(P)H formation are expected to be impaired in pyruvate dehydrogenase deficient strains. As NADH is the source of reduction equivalents for both AlkB and AlaD, a knockout or knockdown of genes with a key role in the central carbon metabolism and especially in NAD(P)H regeneration needs careful evaluation. Hence, a quantitative metabolome and flux analysis under biotransformation conditions may be of interest to evaluate pyruvate node operation.

The pH dependency of AlaD operation may also be a promising engineering target. *In vitro* studies on AlaD revealed an optimum pH of 9 and alanine formation rates were reduced to 20% at pH 7.2 (Yoshida and Freese, 1965). Over an external pH range of 5 – 9, *E. coli* maintains its cytoplasmic pH between 7.4 and 7.8, when optimal growth conditions are applied (Slonczewski et al., 1981; Wilks and Slonczewski, 2007; Zilberstein et al., 1984). Thus, the full potential of AlaD was not exploited for ADAME formation. An AlaD homologue with a pH optimum at neutral pH such as AlaD from *Mycobacterium tuberculosis* (Hutter and Singh, 1999) may be used or protein engineering approaches may be chosen to further improve alanine synthesis and thus ADAME production with engineered *E. coli*.

4.3 Choice of host organism

In general, robustness of microbial cells towards toxic substrates and products as well as the applied process conditions is crucial for commercial process applications in industry (Keasling, 2012; Schmid et al., 2001; Schrewe et al., 2013a). Among the *E. coli* strains tested, *E. coli* BL21 (DE3) carrying AlaD and CV2025 showed the best transamination performance with NH_4Cl as ammonium source, but only in the absence of AlkL and/or AlkBGT. Facilitated uptake via AlkL may cause toxification by substrate and/or products and thus affect cell metabolism and NAD(P)H regeneration compromising AlkBGT and AlaD activity. *E. coli* W3110 and *E. coli* JM101 outperformed *E. coli* BL21 (DE3) in terms of ADAME synthesis from DAME. This is in agreement with the higher robustness of W3110 and especially JM101 towards solvents as it has been shown for styrene oxide (Park et al., 2006). Without induction, the introduction of pAlaDTA and pBTL10 into W3110 and JM101 resulted in a reduction of the exponential growth rate by 70% and 30%, respectively, whereas this effect was not observed for BL21 (DE3) (see supplementary material, Table S1). Growth of all tested strains was further impaired after induction of gene expression, resulting in maximum growth rates of 0.16 and 0.15 h^{-1} for *E. coli* BL21 (DE3) and *E. coli* JM101, respectively, and even in linear growth for *E. coli* W3110. The latter strain obviously was most affected by recombinant gene expression. Thus, among the strains evaluated in this study, *E. coli* JM101 can be considered the strain of choice with regard to robustness towards both organic solvents (substrate/products) and recombinant gene expression.

This study clearly demonstrates that careful host evaluation and selection are essential for efficient bioprocessing based on orthogonal pathways, which typically are highly interconnected with cell functionalities such as carbon and energy metabolism, gene expression, substrate uptake, and robustness towards organic compounds.

448 **4.4 Shift of product formation pattern towards ADAME accumulation**

449 Similar to the xylene monooxygenase of *P. putida* mt-2 (Bühler et al., 2000), AlkBGT does not
450 only catalyze terminal hydroxylation but also the further oxidation of resulting alcohols to
451 corresponding aldehydes and acids (Schrewe et al., 2013b). Regarding the coupling of
452 AlkBGT- and CV2025-catalysis to produce ADAME, ODAME overoxidation constitutes a
453 competing reaction. ODAME accumulated only to low amounts (Fig. 4 A) and its availability,
454 beside that of alanine, obviously limited the transamination reaction during ADAME synthesis
455 from DAME with *E. coli* JM101 (pAlaDTA, pBTL10). Hence, the synthetic pathway was
456 amended by the *P. putida* GPo1 alcohol dehydrogenase AlkJ which is linked to the electron
457 transport chain and thus catalyzes an irreversible alcohol oxidation *in vivo* (Kirmair and Skerra,
458 2014; Schrewe et al., 2014). The introduction of AlkJ was found not only to promote HDAME
459 oxidation but also to favor ADAME over DDAME formation (Fig. 4). Obviously, AlkJ
460 increased the intracellular availability of ODAME fostering CV2025- but not AlkBGT
461 catalysis. This may be due to enzyme kinetics and/or reaction thermodynamics.

462 Regarding ODAME conversion kinetics, the predominance of CV2025 over AlkBGT catalysis
463 as a consequence of the AlkJ-mediated increase in ODAME supply and levels (extracellular
464 concentrations: 0.016 mM without and 0.028 mM with AlkJ, Fig. 4) indicates that both V_{max}
465 and K_M of CV2025 are higher than those of AlkBGT. Indeed, maximal ODAME conversion
466 activities and ODAME uptake constants (K_S values) of AlkL-containing cells in the presence
467 of alanine were clearly higher for CV2025 (623 U g_{CDW}^{-1}, Table 2; subject of substrate
468 inhibition: V_{max} = 3150 ± 1020 U g_{CDW}^{-1}, K_S = 3.2 ± 1.2 mM, , K_i = 1.0 ± 0.4 mM, unpublished
469 data) as comparted to AlkBGT (V_{max} = 103 ± 11 U g_{CDW}^{-1}, K_S = 0.19 ± 0.06 mM, Schrewe et
470 al., 2014). It has to be considered that substrate uptake constants may be dominated by AlkL
471 kinetics and that intracellular enzyme affinities are difficult to judge, especially for membrane
472 bound enzymes such as AlkB, which, however, profits from the high solubility of ODAME in

and its partitioning into membranes. Overall, these kinetic considerations are in agreement with the observed preference for ODAME oxidation and ODAME transamination at low and high ODAME availabilities, respectively.

The thermodynamics of reversible transamination with an equilibrium constant K_{eq} of 134, as estimated via the group contribution method of Mavrovouniotis (1991), may also play a crucial role considering the low ODAME levels in the reaction broth. Accordingly, higher intracellular ODAME concentrations reached in presence of AlkJ can be expected to increase the net ADAME formation rate, whereas irreversible ODAME oxidation by AlkBGT is not influenced by an active back reaction and may already have run at close to maximal speed in the absence of AlkJ. Moreover, ADAME synthesis may become favored over direct further oxidation of ODAME by AlkBGT, if AlkJ rather than AlkBGT (no dissociation of ODAME necessary in this case) catalyzes ODAME formation. However, the favored ADAME formation achieved via the introduction of AlkJ augurs well for the development of a bioprocess featuring predominant ADAME production with renewable DAME as substrate.

Future work will focus on the application of reaction engineering approaches in order to synthesize ADAME on a larger scale. In this respect, the two-liquid phase bioreactor concept represents a good strategy to exploit reaction kinetics and to further increase the product yield (Bühler et al., 2003; Lye and Woodley, 1999; Schrewe et al., 2014).

5. Conclusions

This study reports on the design and engineering of a completely heterologous, rationally compiled pathway involving oxygenase, dehydrogenase, and transaminase catalysis for the production of ADAME, a valuable monomer for Nylon 12 synthesis. To overcome the major limitations for the synthesis ADAME from renewable DAME, strain and pathway engineering targeted hydrophobic substrate uptake, intracellular alanine supply to support transaminase

catalysis, and the introduction of an additional alcohol oxidizing activity to improve pathway flux. Via these strategies, both the specific ADAME formation rate and the yield on biomass were increased 10- and 3.5-fold, respectively. Careful host evaluation and selection as well as the consideration and engineering of general functionalities of microbial cells proved to be crucial to improve the performance of the heterologous pathway. Such cascade biocatalysis based on orthogonal pathway design and engineering constitutes a novel strategy, which enlarges the substrate scope of metabolically engineered microorganisms and finally sets the basis to produce Nylon 12 consisting of 100% renewable carbon.

6. Acknowledgements

We thank the German Federal Ministry of Education and Research (BMBF, grant number 0315205) for financial support.

7. References

Bachmann, B.J., 1987. Derivatisations and genotypes of some mutant derivatives of *Escherichia coli* K-12. American Society for Microbiology, Washington DC.

Blank, L.M., Ebert, B.E., Bühler, B., Schmid, A., 2008. Metabolic capacity estimation of *Escherichia coli* as a platform for redox biocatalysis: constraint-based modeling and experimental verification. Biotechnol. Bioeng. 100, 1050–1065. doi:10.1002/bit.21837

Bühler, B., Bollhalder, I., Hauer, B., Witholt, B., Schmid, A., 2003. Use of the two-liquid phase concept to exploit kinetically controlled multistep biocatalysis. Biotechnol. Bioeng. 81, 683–694. doi:10.1002/bit.10512

Bühler, B., Schmid, A., Hauer, B., Witholt, B., 2000. Xylene Monooxygenase catalyzes the multistep oxygenation of toluene and pseudocumene to corresponding alcohols, aldehydes, and acids in *Escherichia coli* JM101. J. Biol. Chem. 275, 10085–10092. doi:10.1074/jbc.275.14.10085

Carole, T.M., Pellegrino, J., Paster, M.D., 2004. Opportunities in the Industrial Biobased Products Industry. Appl. Biochem. Biotechnol. 115, 0871–0886. doi:10.1385/ABAB:115:1-3:0871

527 Chen, R., 2007. Permeability issues in whole-cell bioprocesses and cellular membrane
528 engineering. Appl. Microbiol. Biotechnol. 74, 730–738. doi:10.1007/s00253-006-0811-x
529 Cornelissen, S., Julsing, M.K., Volmer, J., Riechert, O., Schmid, A., Bühler, B., 2013. Whole-
530 cell-based CYP153A6-catalyzed (S)-limonene hydroxylation efficiency depends on host
531 background and profits from monoterpene uptake via AlkL. Biotechnol. Bioeng. 110,
532 1282–1292. doi:10.1002/bit.24801
533 Curran, K.A., Leavitt, J.M., Karim, A.S., Alper, H.S., 2013. Metabolic engineering of muconic
534 acid production in *Saccharomyces cerevisiae*. Metab. Eng. 15, 55–66.
535 doi:10.1016/j.ymben.2012.10.003
536 Dachs, K., Schwartz, E., 1962. Pyrrolidon, Capryllactam und Laurinlactam als neue
537 Grundstoffe für Polyamidfasern. Angew. Chem. 74, 540–545.
538 doi:10.1002/ange.19620741505
539 Franke, W.K., Müller, K.-A., 1964. Synthesewege zum Laurinlactam für Nylon 12. Chem. Ing.
540 Tech. - CIT 36, 960–962. doi:10.1002/cite.330360911
541 Evonik Industries, 2015, http://www.vestamid.com/product/vestamid/en/Pages/default.aspx;
542 date: 15.04.2015
543 Hanahan, D., 1983. Studies on transformation of *Escherichia coli* with plasmids. J. Mol. Biol.
544 166, 557–580. doi:10.1016/S0022-2836(83)80284-8
545 Hutter, B., Singh, M., 1999. Properties of the 40 kDa antigen of *Mycobacterium tuberculosis*,
546 a functional L-alanine dehydrogenase. Biochem. J. 343, 669–672.
547 Julsing, M.K., Schrewe, M., Cornelissen, S., Hermann, I., Schmid, A., Bühler, B., 2012. Outer
548 membrane protein AlkL boosts biocatalytic oxyfunctionalization of hydrophobic substrates
549 in *Escherichia coli*. Appl. Environ. Microbiol. 78, 5724–5733. doi:10.1128/AEM.00949-
550 12
551 Kaulmann, U., Smithies, K., Smith, M.E.B., Hailes, H.C., Ward, J.M., 2007. Substrate spectrum
552 of ω-transaminase from *Chromobacterium violaceum* DSM30191 and its potential for
553 biocatalysis. Enzyme Microb. Technol. 41, 628–637. doi:10.1016/j.enzmictec.2007.05.011
554 Keasling, J.D., 2012. Synthetic biology and the development of tools for metabolic engineering.
555 Metab. Eng. 14, 189–195. doi:10.1016/j.ymben.2012.01.004
556 Kind, S., Neubauer, S., Becker, J., Yamamoto, M., Völkert, M., Abendroth, G. von, Zelder, O.,
557 Wittmann, C., 2014. From zero to hero – Production of bio-based nylon from renewable
558 resources using engineered Corynebacterium glutamicum. Metab. Eng. 25, 113–123.
559 doi:10.1016/j.ymben.2014.05.007
560 Kirmair, L., Skerra, A., 2014. Biochemical analysis of recombinant AlkJ from *Pseudomonas*

putida reveals a membrane-associated, FAD-dependent dehydrogenase suitable for the biosynthetic production of aliphatic aldehydes. Appl. Environ. Microbiol. 8, 2468–2477. doi:10.1128/AEM.04297-13

Kuhn, D., Fritzsch, F.S.O., Zhang, X., Wendisch, V.F., Blank, L.M., Bühler, B., Schmid, A., 2013. Subtoxic product levels limit the epoxidation capacity of recombinant *E. coli* by increasing microbial energy demands. J. Biotechnol. 163, 194–203. doi:10.1016/j.jbiotec.2012.07.194

Laemmli, U.K., 1970. Cleavage of structural proteins during assemly of the head of bateriophage T4. Nature 227, 680–685. doi:10.1038/227680a0

Lee, M., Smith, G.M., Eiteman, M.A., Altman, E., 2004. Aerobic production of alanine by *Escherichia coli aceF ldhA* mutants expressing the *Bacillus sphaericus alaD* gene. Appl. Microbiol. Biotechnol. 65, 56–60. doi:10.1007/s00253-004-1560-3

Lee, S.Y., Park, S.H., Hong, S.H., Lee, Y., Lee, S.H., 2005. Fermentative Production of Building Blocks for Chemical Synthesis of Polyesters, in: Steinbüchel, A. (Ed.), Biopolymers Online. Wiley-VCH Verlag GmbH & Co. KGaA, Weinheim, Germany.

Leive, L., 1974. The barrier function of the gram-negative envelope. Ann. N. Y. Acad. Sci. 235, 109–129. doi:10.1111/j.1749-6632.1974.tb43261.x

Lye, G., Woodley, J.M., 1999. Application of in situ product-removal techniques to biocatalytic processes. Trends Biotechnol. 17, 395–402. doi:10.1016/S0167-7799(99)01351-7

Mavrovouniotis, M.L., 1991. Estimation of standard Gibbs energy changes of biotransformations. J. Biol. Chem. 266, 14440–14445.

Messing, J., 1979. A multi-purpose cloning system based on the single stranded bacteriophage M13. Recomb. DNA Tech. Bull. 79-99, 42–48.

Nieboer, M., Vis, A.-J., Witholt, B., 1996. Overproduction of a foreign membrane protein in *Escherichia coli* stimulates and depends on phospholipid synthesis. Eur. J. Biochem. 241, 691–696. doi:10.1111/j.1432-1033.1996.00691.x

Nikaido, H., 2003. Molecular basis of bacterial outer membrane permeability revisited. Microbiol. Rev. 67, 593–656. doi:0.1128/MMBR.67.4.593-656.2003

Niu, W., Draths, K.M., Frost, J.W., 2002. Benzene-free synthesis of adipic acid. Biotechnol. Prog. 18, 201–211. doi:10.1021/bp010179x

Oberleitner, N., Peters, C., Muschiol, J., Kadow, M., Saß, S., Bayer, T., Schaaf, P., Iqbal, N., Rudroff, F., Mihovilovic, M.D., Bornscheuer, U.T., 2013. An enzymatic toolbox for cascade reactions: A showcase for an *in vivo* redox sequence in asymmetric synthesis. ChemCatChem 5, 3524–3528. doi:10.1002/cctc.201300604

595 Palmer, R.J., 2001. Polyamides, Plastics, in: Encyclopedia of Polymer Science and Technology.
596 John Wiley & Sons, Inc., Hoboken, NJ, USA.
597 Panke, S., Meyer, A., Huber, C.M., Witholt, B., Wubbolts, M.G., 1999. An alkane-responsive
598 expression system for the production of fine chemicals. Appl. Environ. Microbiol. 65,
599 2324–2332.
600 Park, J.-B., Bühler, B., Habicher, T., Hauer, B., Panke, S., Witholt, B., Schmid, A., 2006. The
601 efficiency of recombinant *Escherichia coli* as biocatalyst for stereospecific epoxidation.
602 Biotechnol. Bioeng. 95, 501–512. doi:10.1002/bit.21037
603 Pramanik, J., Keasling, J.D., 1997. Stoichiometric model of *Escherichia coli* metabolism:
604 Incorporation of growth-rate dependent biomass composition and mechanistic energy
605 requirements. Biotechnol. Bioeng. 56, 398–421. doi:10.1002/(SICI)1097-
606 0290(19971120)56:4<398::AID-BIT6>3.0.CO;2-J
607 Sambrook, J., 2001. Molecular cloning: A laboratory manual. Cold Spring Harbor Laboratory
608 Press, Cold Spring Harbor, NY.
609 Sattler, J.H., Fuchs, M., Tauber, K., Mutti, F.G., Faber, K., Pfeffer, J., Haas, T., Kroutil, W.,
610 2012. Redox self-sufficient biocatalyst network for the amination of primary alcohols.
611 Angew. Chem. Int. Ed. 51, 9156–9159. doi:10.1002/anie.201204683
612 Scheps, D., Honda Malca, S., Richter, S.M., Marisch, K., Nestl, B.M., Hauer, B., 2013.
613 Synthesis of ω-hydroxy dodecanoic acid based on an engineered CYP153A fusion
614 construct: Biocatalytic fatty acid omega-hydroxylation. Microb. Biotechnol. 6, 694–707.
615 doi:10.1111/1751-7915.12073
616 Schmid, A., Dordick, J.S., Hauer, B., Kiender, M., Wubbolts, M., Witholt, B., 2001. Industrial
617 biocatalysis today and tomorrow. Nature 409, 258–268.
618 Schmitz, K., Schepers, U., 2004. Polyamides as artificial transcription factors: novel tools for
619 molecular medicine? Angew. Chem. Int. Ed. 43, 2472–2475. doi:10.1002/anie.200301745
620 Schrewe, M., Julsing, M.K., Bühler, B., Schmid, A., 2013a. Whole-cell biocatalysis for
621 selective and productive C–O functional group introduction and modification. Chem. Soc.
622 Rev. 42, 6346–6377. doi:10.1039/c3cs60011d
623 Schrewe, M., Julsing, M.K., Lange, K., Czarnotta, E., Schmid, A., Bühler, B., 2014. Reaction
624 and catalyst engineering to exploit kinetically controlled whole-cell multistep biocatalysis
625 for terminal FAME oxyfunctionalization. Biotechnol. Bioeng. doi:10.1002/bit.25248
626 Schrewe, M., Ladkau, N., Bühler, B., Schmid, A., 2013b. Direct terminal alkylamino-
627 functionalization *via* multistep biocatalysis in one recombinant whole-cell catalyst. Adv.
628 Synth. Catal. 355, 1693–1697. doi:10.1002/adsc.201200958

Schrewe, M., Magnusson, A.O., Willrodt, C., Bühler, B., Schmid, A., 2011. Kinetic analysis of terminal and unactivated C-H bond oxyfunctionalization in fatty acid methyl esters by monooxygenase-based whole-cell biocatalysis. Adv. Synth. Catal. 353, 3485–3495. doi:10.1002/adsc.201100440

Slonczewski, J.L., Rosen, B.P., Alger, J.R., Macnab, R.M., 1981. pH homeostasis in *Escherichia coli*: measurement by 31P nuclear magnetic resonance of methylphosphonate and phosphate. Proc. Natl. Acad. Sci. U. S. A. 78, 6271–6275.

Smith, G., Lee, S., Reilly, K., Eiteman, M., Altman, E., 2006. Fed-batch two-phase production of alanine by a metabolically engineered *Escherichia coli*. Biotechnol. Lett. 28, 1695–1700. doi:10.1007/s10529-006-9142-3

Smits, T.H.M., Seeger, M.A., Witholt, B., van Beilen, J.B., 2001. New alkane-responsive expression vectors for *Escherichia coli* and Pseudomonas. Plasmid 46, 16–24. doi:10.1006/plas.2001.1522

Song, J.-W., Jeon, E.-Y., Song, D.-H., Jang, H.-Y., Bornscheuer, U.T., Oh, D.-K., Park, J.-B., 2013. Multistep enzymatic synthesis of long-chain α,ω-dicarboxylic and ω-hydroxycarboxylic acids from renewable fatty acids and plant oils. Angew. Chem. Int. Ed. 52, 2534–2537. doi:10.1002/anie.201209187

Stark, D., von Stockar, U., 2003. In situ product removal (ISPR) in whole cell biotechnology during the last twenty years, in: von Stockar, U., Wielen, L.A.M., Bruggink, A., Cabral, J.M.S., Enfors, S.-O., Fernandes, P., Jenne, M., Mauch, K., Prazeres, D.M.F., Reuss, M., Schmalzriedt, S., Stark, D., Stockar, U., Straathof, A.J.J., Wielen, L.A.M. (Eds.), Process Integration in Biochemical Engineering, Advances in Biochemical Engineering/Biotechnology. Springer Berlin Heidelberg, Berlin, Heidelberg, pp. 149–175.

Studier, F.W., Moffatt, B.A., 1986. Use of bacteriophage T7 RNA polymerase to direct selective high-level expression of cloned genes. J. Mol. Biol. 189, 113–130. doi:10.1016/0022-2836(86)90385-2

Wilks, J.C., Slonczewski, J.L., 2007. pH of the cytoplasm and periplasm of *Escherichia coli*: Rapid measurement by green fluorescent protein fluorimetry. J. Bacteriol. 189, 5601–5607. doi:10.1128/JB.00615-07

Yoshida, A., Freese, E., 1965. Enzymic properties of alanine dehydrogenase of *Bacillus subtilis*. Biochim. Biophys. Acta 96, 248–263. doi:http://dx.doi.org/10.1016/0926-6593(65)90009-3

Zilberstein, D., Agmon, V., Schuldiner, S., Padan, E., 1984. *Escherichia coli* intracellular pH, membrane potential, and cell growth. J. Bacteriol. 158, 246–252.

Supplementary Material

Efficient production of the Nylon 12 monomer ω-aminododecanoic acid methyl ester from renewable dodecanoic acid methyl ester with engineered *Escherichia coli*

Nadine Ladkau[a,1], Miriam Assmann[a,2], Manfred Schrewe[a,b], Mattijs K. Julsing[a], Andreas Schmid[a,b,*], and Bruno Bühler[a,b,*]

[a] Laboratory of Chemical Biotechnology, Department of Biochemical and Chemical Engineering, TU Dortmund University, Emil-Figge-Strasse 66, 44227 Dortmund, Germany.

[b] Department of Solar Materials, Helmholtz Centre for Environmental Research – UFZ, Permoserstrasse 15, 04318 Leipzig, Germany.

[1] Current address: Department of Chemistry, University College London, 20 Gordon Street, WC1H 0AJ London, UK.

[2] Current address: Institute of Technical Biocatalysis, Technical University Hamburg-Harburg, Denickestrasse 15, 21073 Hamburg, Germany

Corresponding authors:

Phone: +49 341 235 1286, Fax: +49 341 235 451286, E-mail: andreas.schmid@ufz.de;

Phone: +49 341 235 4687; Fax: +49 341 235 451286, E-mail: bruno.buehler@ufz.de

Contents:

I. DNA and amino acid sequence of *alaD* on plasmid pAlaDTA

II. DNA and amino acid sequence of *ω-TA* on pAlaDTA

III. Supplementary table

IV. Supplementary figures

I. DNA and amino acid sequence of *B. subtilis alaD* on plasmid pAlaDTA

DNA sequence:

ATGATCATAGGGGTTCCTAAAGAGATAAAAAACAATGAAAACCGTGTCGCATTAACACC
CGGGGGCGTTTCTCAGCTCATTTCAAACGGCCACCGGGTGCTGGTTGAAACAGGCGCGGG
CCTTGGAAGCGGATTTGAAAATGAAGCCTATGAGTCAGCAGGAGCGGAAATCATTGCTG
ATCCGAAGCAGGTCTGGGACGCCGAAATGGTCATGAAAGTAAAAGAACCGCTGCCGGAA
GAATATGTTTATTTTCGCAAAGGACTTGTGCTGTTTACGTACCTTCATTTAGCAGCTGAGC
CTGAGCTTGCACAGGCCTTGAAGGATAAAGGAGTAACTGCCATCGCATATGAAACGGTC
AGTGAAGGCCGGACATTGCCTCTTCTGACGCCAATGTCAGAGGTTGCGGGCAGAATGGCA
GCGCAAATCGGCGCTCAATTCTTAGAAAAGCCTAAAGGCGGAAAAGGCATTCTGCTTGCC
GGGGTGCCTGGCGTTTCCCGCGGAAAAGTAACAATTATCGGAGGAGGCGTTGTCGGGAC
AAACGCGGCGAAAATGGCTGTCGGCCTCGGTGCAGATGTGACGATCATTGACTTAAACGC
AGACCGCTTGCGCCAGCTTGATGACATCTTCGGCCATCAGATTAAAACGTTAATTTCTAAT
CCGGTCAATATTGCTGATGCTGTGGCGGAAGCGGATCTCCTCATTTGCGCGGTATTAATTC
CGGGTGCTAAAGCTCCGACTCTTGTCACTGAGGAAATGGTAAAACAAATGAAACCCGGTT
CAGTTATTGTTGATGTAGCGATCGACCAAGGCGGCATCGTCGAAACTGTCGACCATATCA
CAACACATGATCAGCCAACATATGAAAAACACGGGGTTGTGCATTATGCTGTAGCGAAC
ATGCCAGGCGCAGTCCCTCGTACATCAACAATCGCCCTGACTAACGTTACTGTTCCATAC
GCGCTGCAAATCGCGAACAAAGGGGCAGTAAAAGCGCTCGCAGACAATACGGCACTGAG
AGCGGGTTTAAACACCGCAAACGGACACGTGACCTATGAAGCTGTAGCAAGAGATCTAG
GCTATGAGTATGTTCCTGCCGAGAAAGCTTTACAGGATGAATCATCTGTGGCGGGTGCTT
AA

Amino acid sequence:

MIIGVPKEIKNNENRVALTPGGVSQLISNGHRVLVETGAGLGSGFENEAYESAGAEIIADPKQV
WDAEMVMKVKEPLPEEYVYFRKGLVLFTYLHLAAEPELAQALKDKGVTAIAYETVSEGRTL
PLLTPMSEVAGRMAAQIGAQFLEKPKGGKGILLAGVPGVSRGKVTIIGGGVVGTNAAKMAV
GLGADVTIIDLNADRLRQLDDIFGHQIKTLISNPVNIADAVAEADLLICAVLIPGAKAPTLVTEE
MVKQMKPGSVIVDVAIDQGGIVETVDHITTHDQPTYEKHGVVHYAVANMPGAVPRTSTIALT
NVTVPYALQIANKGAVKALADNTALRAGLNTANGHVTYEAVARDLGYEYVPAEKALQDES
SVAGA

II. DNA and amino acid sequence of codon optimized *cv2025* ω-TA from *C. violaceum* on pAlaDTA

DNA sequence:

ATGCAGAAACAGCGTACCACCTCTCAGTGGCGTGAACTCGATGCGGCGCATCATCTCCAT
CCGTTTACCGATACCGCGAGCCTCAATCAGGCGGGTGCGCGTGTGATGACCCGTGGCGAA
GGCGTGTATCTCTGGGATAGCGAAGGCAACAAAATTATTGATGGCATGGCGGGCCTCTGG
TGCGTGAACGTGGGCTATGGCCGTAAAGATTTTGCGGAAGCGGCGCGTCGTCAGATGGA
AGAACTCCCGTTTTATAACACCTTCTTTAAAACCACCCATCCGGCGGTGGTGGAACTCAG
CAGCCTCCTCGCCGAAGTTACCCCGGCAGGTTTTGATCGTGTGTTTTATACCAACAGCGGC
AGCGAAAGCGTGGATACCATGATTCGTATGGTGCGTCGTTATTGGGATGTGCAGGGCAAA
CCGGAAAAAAAAAACCCTCATTGGCCGTTGGAACGGCTATCACGGCAGCACCATTGGCGG
TGCGAGCCTCGGCGGCATGAAATATATGCATGAACAGGGCGATCTCCCGATTCCGGGCAT
GGCGCATATTGAACAGCCGTGGTGGTATAAACATGGCAAAGATATGACCCCGGATGAAT
TTGGCGTGGTTGCGGCGCGTTGGCTCGAAGAAAAAATTCTCGAAATCGGCGCGGATAAA
GTGGCGGCGTTTGTGGGCGAACCGATTCAGGGTGCGGGCGGTGTGATTGTTCCGCCGGCA
ACCTATTGGCCGGAAATTGAACGTATTTGCCGCAAATATGATGTGCTCCTCGTTGCGGAT
GAAGTGATTTGCGGCTTTGGCCGTACCGGCGAATGGTTTGGCCATCAGCATTTTGGCTTTC
AGCCGGACCTCTTTACCGCGGCGAAAGGCCTCAGCAGCGGCTATCTCCCGATTGGCGCGG
TGTTTGTGGGCAAACGTGTTGCGGAAGGTCTCATTGCGGGCGGTGATTTTAACCATGGCT
TTACCTATAGCGGCCATCCGGTGTGTGCGGCGGTGGCGCATGCGAATGTTGCGGCGCTCC
GTGATGAAGGCATTGTGCAGCGTGTGAAAGATGATATTGGCCCGTATATGCAGAAACGTT
GGCGTGAAACCTTTAGCCGTTTTGAACATGTGGATGATGTGCGTGGCGTGGGCATGGTGC
AGGCGTTTACCCTCGTGAAAAACAAAGCGAAACGTGAACTCTTTCCGGATTTTGGCGAAA
TTGGCACCCTCTGCCGCGATATTTTTTTTCGCAACAACCTCATTATGCGTGCGTGCGGCGA
TCACATTGTGTCTGCACCGCCGCTCGTTATGACCCGTGCGGAAGTGGATGAAATGCTCGC
CGTGGCGGAACGTTGCCTCGAAGAATTTGAACAGACCCTCAAAGCGCGTGGCCTCGCCTA
A

Amino acid sequence:

MQKQRTTSQWRELDAAHHLHPFTDTASLNQAGARVMTRGEGVYLWDSEGNKIIDGMAGLW
CVNVGYGRKDFAEAARRQMEELPFYNTFFKTTHPAVVELSSLLAEVTPAGFDRVFYTNSGSE
SVDTMIRMVRRYWDVQGKPEKKTLIGRWNGYHGSTIGGASLGGMKYMHEQGDLPIPGMAH
IEQPWWYKHGKDMTPDEFGVVAARWLEEKILEIGADKVAAFVGEPIQGAGGVIVPPATYWP
EIERICRKYDVLLVADEVICGFGRTGEWFGHQHFGFQPDLFTAAKGLSSGYLPIGAVFVGKRV
AEGLIAGGDFNHGFTYSGHPVCAAVAHANVAALRDEGIVQRVKDDIGPYMQKRWRETFSRF
EHVDDVRGVGMVQAFTLVKNKAKRELFPDFGEIGTLCRDIFFRNNLIMRACGDHIVSAPPLV
MTRAEVDEMLAVAERCLEEFEQTLKARGLA

III. Supplementary table

The growth behavior of recombinant *E. coli* carrying either the plasmid pAlaDTA or the plasmids pAlaDTA/pBTL10 was investigated in M9* minimal medium at 30°C. Induction was carried out with 1mM IPTG for strains carrying pAlaDTA or with 0.025% when pBTL10 was present in the cells.

Table S1 Maximum growth rates (μ_{max} [h^{-1}]) of recombinant *E. coli* strains carrying pAlaDTA or pAlaDTA in combination with pBTL10.

	w/o plasmid	pAlaDTA		pAlaDTA/pBTL10	
µmax [h^{-1}]		uninduced	induced[a)]	uninduced	induced[b)]
BL21 (DE3)	0.38±0.05	0.35±0.04	0.35±0.05	0.39±0.05	0.16±0.05
W3110	0.55±0.08	0.33±0.05	0.28±0.06	0.16±0.03	linear
JM101	0.47±0.09	0.40±0.06	0.38±0.05	0.33±0.04	0.15±0.03

Induction was performed after growing the cells to a concentration of 0.083 g_{CDW} L^{-1}.

[a)] induction with 1 mM IPTG

[b)] induction with 1mM IPTG and 0.025% DCPK

IV. Supplementary figures

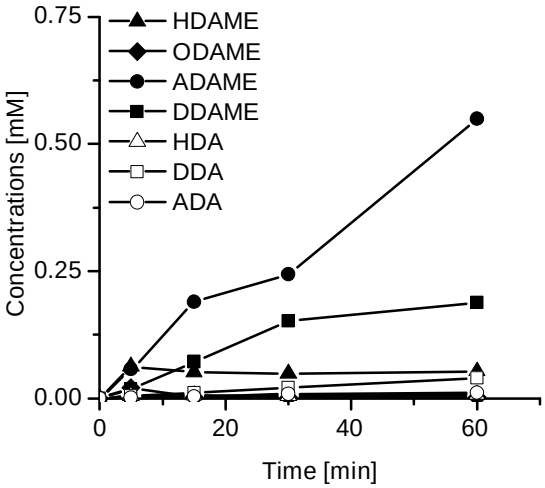

Fig. S1: Hydrolyzed and non-hydrolyzed alcohol, aldehyde (not detected), acid, and amine products accumulating during the whole-cell biotransformation of DAME shown in Fig. 2 with *E. coli* BL21 (DE3) (pTA, pBTL10). Cell concentration applied: 1.25 g_{CDW} L^{-1}. Kpi buffer was supplemented with 50 mM L-alanine. HDAME, 12-hydroxydodecanoic acid methyl ester; ODAME, 12-oxododecanoic acid methyl ester; DDAME, dodecanedioic acid monomethyl ester; ADAME, 12-aminododecanoic acid methyl ester; HAD, 12-hydroxydodecanoic acid; DDA, dodecanedioic acid; ADA, 12-aminododecanoic acid.

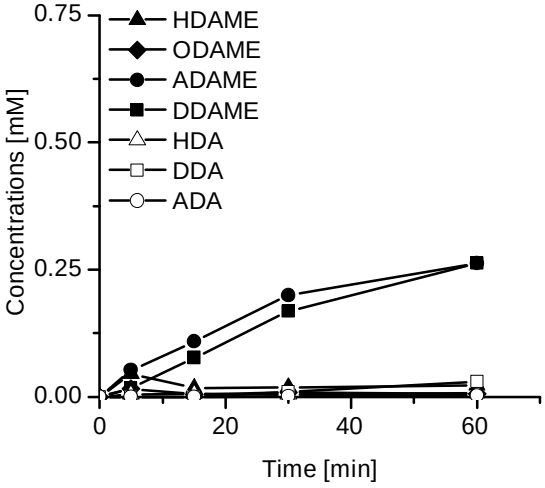

Fig. S2: Hydrolyzed and non-hydrolyzed alcohol, aldehyde (not detected), acid, and amine products accumulated during the whole-cell biotransformation of DAME shown in Fig. 4AB with *E. coli* JM101 (pAlaDTA, pBTL10). Cell concentration applied: 0.64 g_{CDW} L^{-1}. Kpi buffer was supplemented with 15 g L^{-1} NH_4Cl. Abbreviations are as given in the legend of Fig. S1.

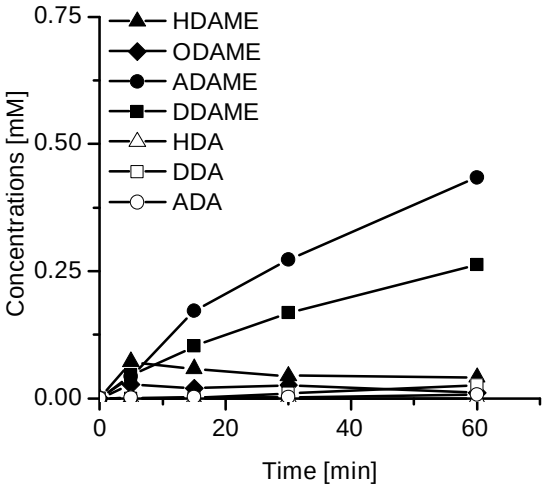

Fig. S3: Hydrolyzed and non-hydrolyzed alcohol, aldehyde (not detected), acid and amine products accumulated during the whole-cell biotransformation of DAME shown in Fig 4CD with *E. coli* JM101 (pAlaDTA, pBTJL10). Cell concentration applied: 0.64 g_{CDW} L^{-1}. Kpi buffer was supplemented with 15 g L^{-1} NH_4Cl. Abbreviations are as given in the legend of Fig. S1.

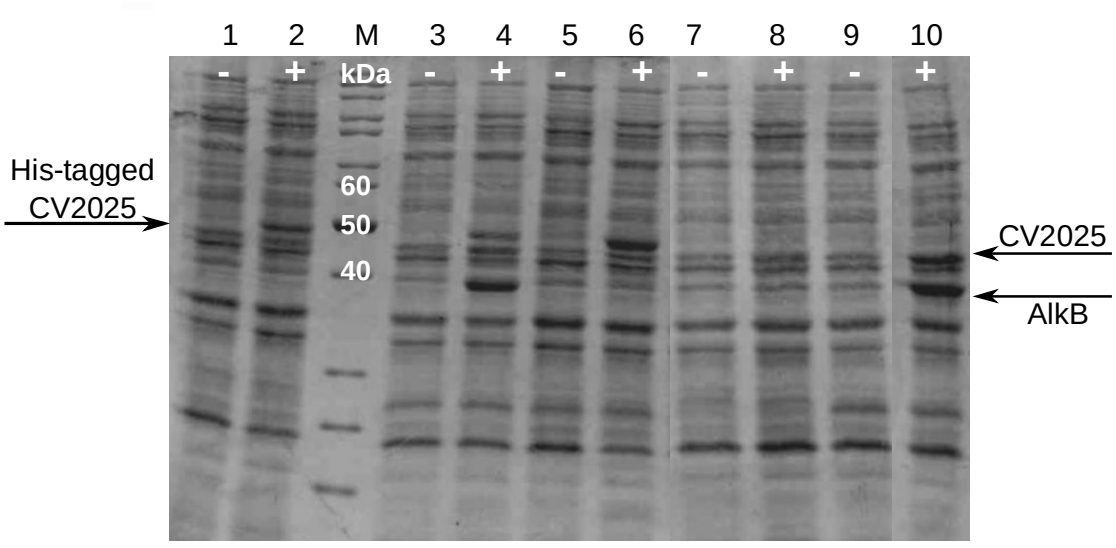

Fig. S4: SDS-PAGE analysis of recombinant *E. coli* BL21 (DE3) carrying different plasmids. pTA in lanes 1 and 2, pTA and pBTL10 in lanes 3 and 4, pTA and pCom10alkL in lanes 5 and 6, pAlaDTA in lanes 7 and 8, and pAlaDTA and pBTL10 in lanes 9 and10. Lane M, PageRuler SM26614 (Fermentas GmbH, St. Leon-Rot, Germany). "-" = uninduced cultures, "+" = after 5 h of induction. Induction was carried out with 1 mM IPTG for strains carrying the plasmids pTA or pAlaDTA and with 0.025% (v/v) DCPK for strains harboring pBTL10. Approx.15 µg of total cell dry weight was loaded. Expected molecular mass: CV2025: ~ 47 kDa (Kaulmann et al., 2007), AlaD: ~ 42 kDa (Ye et al., 2010); AlkB: ~ 41 kDa (Schrewe et al., 2011).

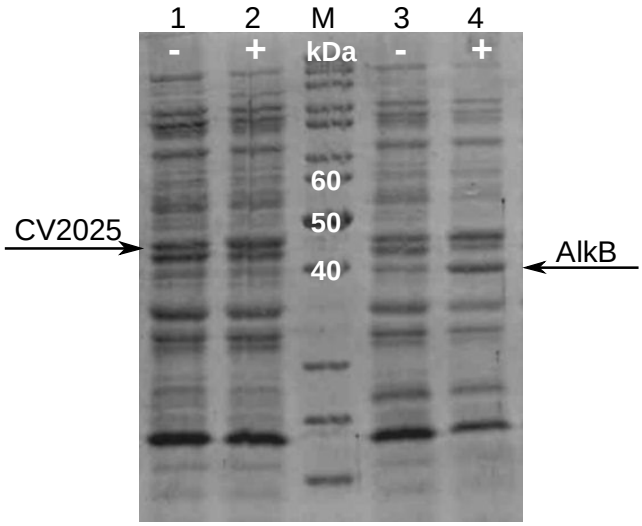

Fig. S5: SDS-PAGE analysis of recombinant *E. coli* W3110 carrying different plasmids. pAlaDTA in lanes 1 and 2, pAlaDTA and pBTL10 in lanes 3 and 4. Lane M, PageRuler SM26614 (Fermentas GmbH, St. Leon-Rot, Germany). "-" = uninduced cultures, "+" = after 5 h of induction. Induction was carried out with 1 mM IPTG for strains carrying the plasmid pAlaDTA and with 0.025% (v/v) DCPK for strains harboring pBTL10. Approx.15 µg of total cell dry weight was loaded. Expected molecular mass: CV2025: ~ 47 kDa (Kaulmann et al., 2007), AlaD: ~ 42 kDa (Ye et al., 2010); AlkB: ~ 41 kDa (Schrewe et al., 2011).

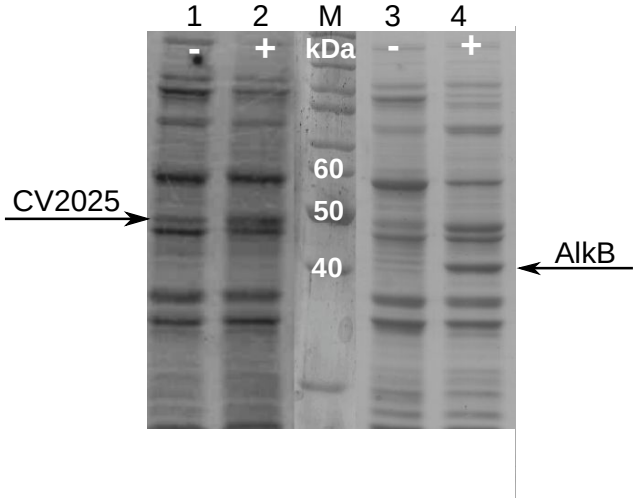

Fig. S6: SDS-PAGE analysis of recombinant *E. coli* JM101 carrying different plasmids. pAlaDTA in lanes 1 and 2, pAlaDTA and pBTL10 in lanes 3 and 4. M: PageRuler SM26614 (Fermentas GmbH, St. Leon-Rot, Germany). "-" = uninduced cultures, "+" = after 5 h of

induction. Induction was carried out with 1 mM IPTG for strains carrying the plasmid pAlaDTA and with 0.025% (v/v) DCPK for strains harboring pBTL10. Approx.15 µg of total cell dry weight was loaded. Expected molecular mass: CV2025: ~ 47 kDa (Kaulmann et al., 2007), AlaD: ~ 42 kDa (Ye et al., 2010); AlkB: ~ 41 kDa (Schrewe et al., 2011).

References

Kaulmann, U., Smithies, K., Smith, M.E.B., Hailes, H.C., Ward, J.M., 2007. Substrate spectrum of ω-transaminase from *Chromobacterium violaceum* DSM30191 and its potential for biocatalysis. Enzyme Microb. Technol. 41, 628–637. doi:10.1016/j.enzmictec.2007.05.011

Schrewe, M., Magnusson, A.O., Willrodt, C., Bühler, B., Schmid, A., 2011. Kinetic analysis of terminal and unactivated C-H bond oxyfunctionalization in fatty acid methyl esters by monooxygenase-based whole-cell biocatalysis. Adv. Synth. Catal. 353, 3485–3495. doi:10.1002/adsc.201100440

Ye, W., Huo, G., Chen, J., Liu, F., Yin, J., Yang, L., Ma, X., 2010. Heterologous expression of the *Bacillus subtilis* (natto) alanine dehydrogenase in *Escherichia coli* and *Lactococcus lactis*. Microbiol. Res. 165, 268–275. doi:10.1016/j.micres.2009.05.008

Graphical Abstract